Supporting Information for 'Histone titration against the genome sets the DNA-to-cytoplasm threshold for the *Xenopus* midblastula transition'

Amanda A. Amodeo, David Jukam, Aaron F. Straight & Jan M. Skotheim

Table of Contents

Supplemental Figures:
Fig. S1

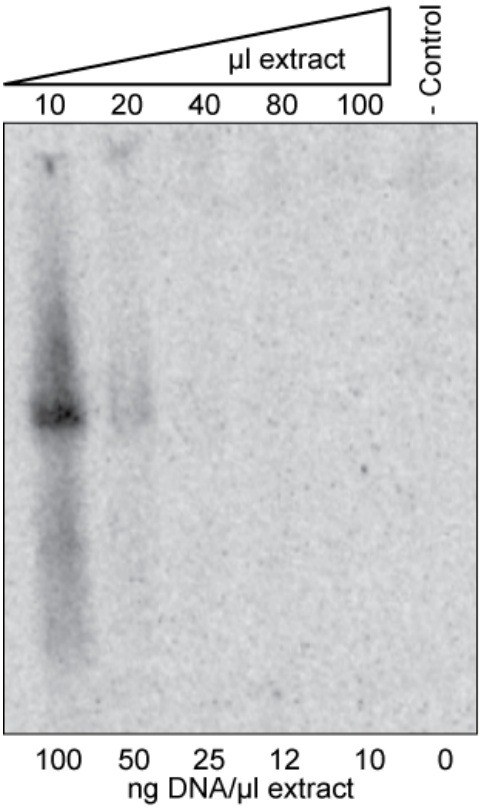

Fig. S1. DNA-to-cytoplasm ratio controls transcription. Extract volume was varied (as labeled on top x-axis) while the quantity of sperm chromatin was kept constant (1µg per sample), resulting in indicated ratios (bottom x-axis) of DNA-to-cytoplasm without varying the quantity of template. Reactions containing smaller volumes of extract resulted in greater total transcription.

Fig. S2

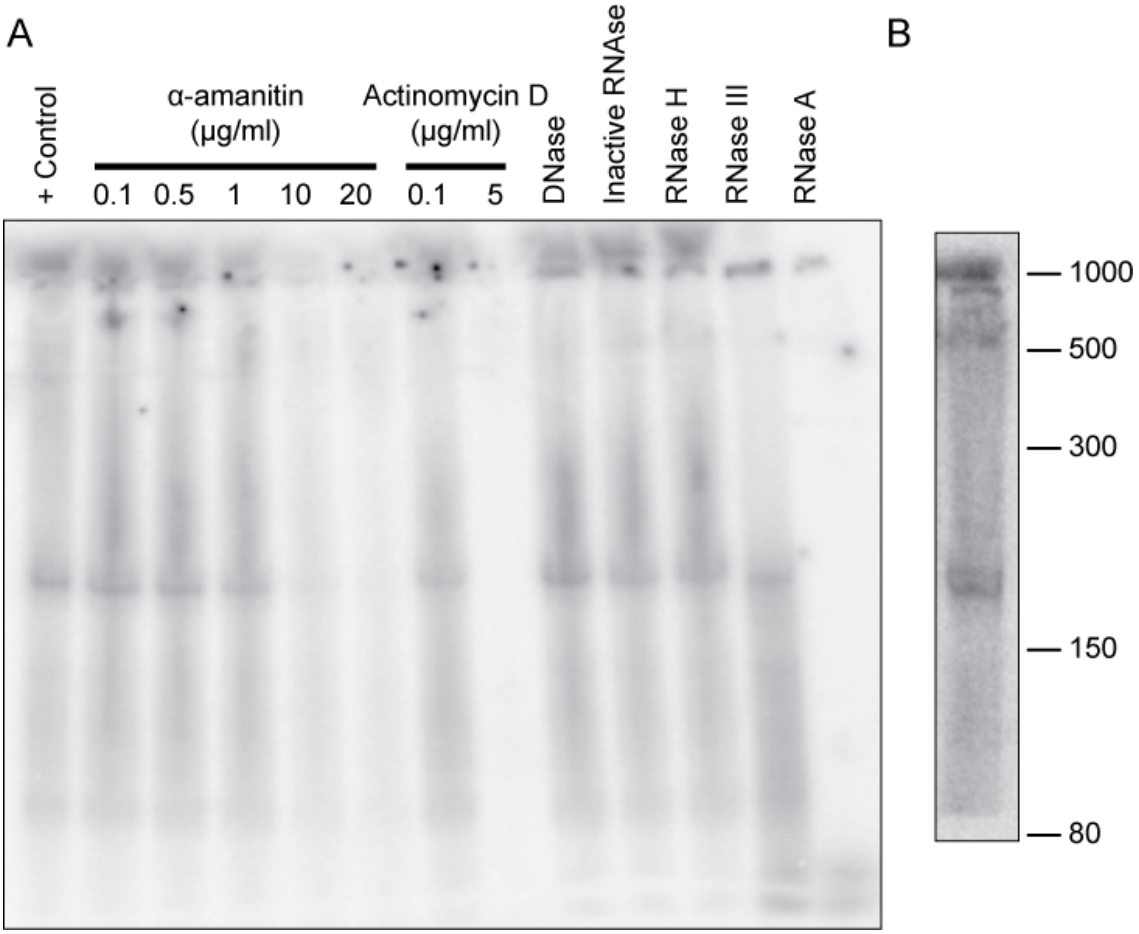

Fig. S2. The major sperm chromatin transcript is a single stranded Pol III product**.** (*A*) Concentrations of α-amanitin or actinomycin D as indicated were added during the transcription reaction. The low sensitivity of our product to both inhibitors indicates that it is likely an RNA Polymerase III transcript. The purified RNA was incubated with DNase, inactive RNase H-D10A, RNase H, RNase III, or RNase A and showed the greatest sensitivity to RNase A indicating that the product is likely single stranded. (*B*) An autoradiograph with molecular weight markers indicating that the major transcript is approximately 180-220 nucleotides.

Fig. S3

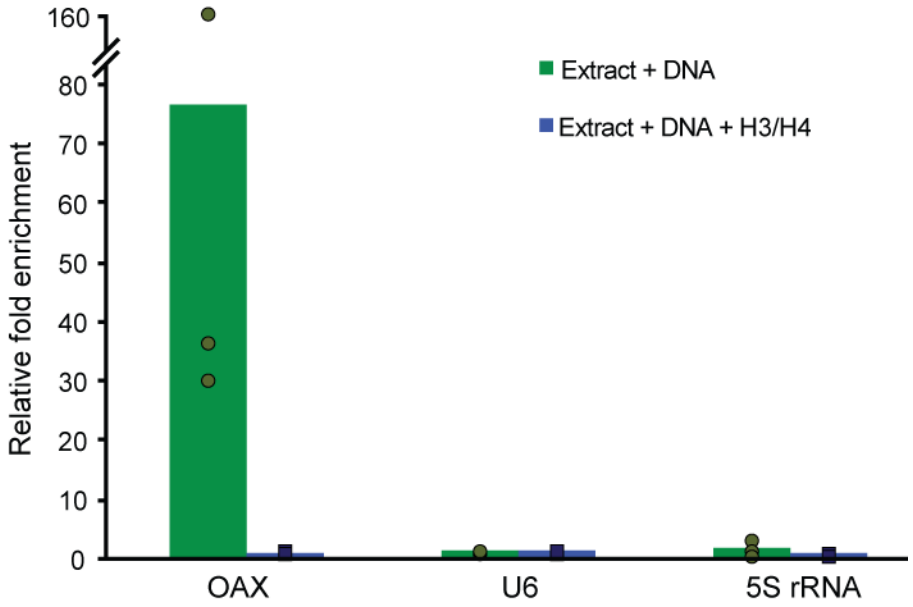

Fig. S3. The major sperm chromatin transcript is OAX. Sperm concentrations above threshold result in a >70-fold increase in OAX transcription over control samples containing α-amanitin or actinomycin D and the same amount of DNA, whereas two other Pol III transcripts of less than 250nt, U6 and 5S-RNA, are not highly expressed off of sperm chromatin in extract (green bars) by qPCR. Addition of exogenous H3/H4 inhibits transcription of OAX from sperm chromatin (blue bars). Fold enrichment is plotted for 2-3 independent experiments (green circles and blue boxes).

Fig. S4

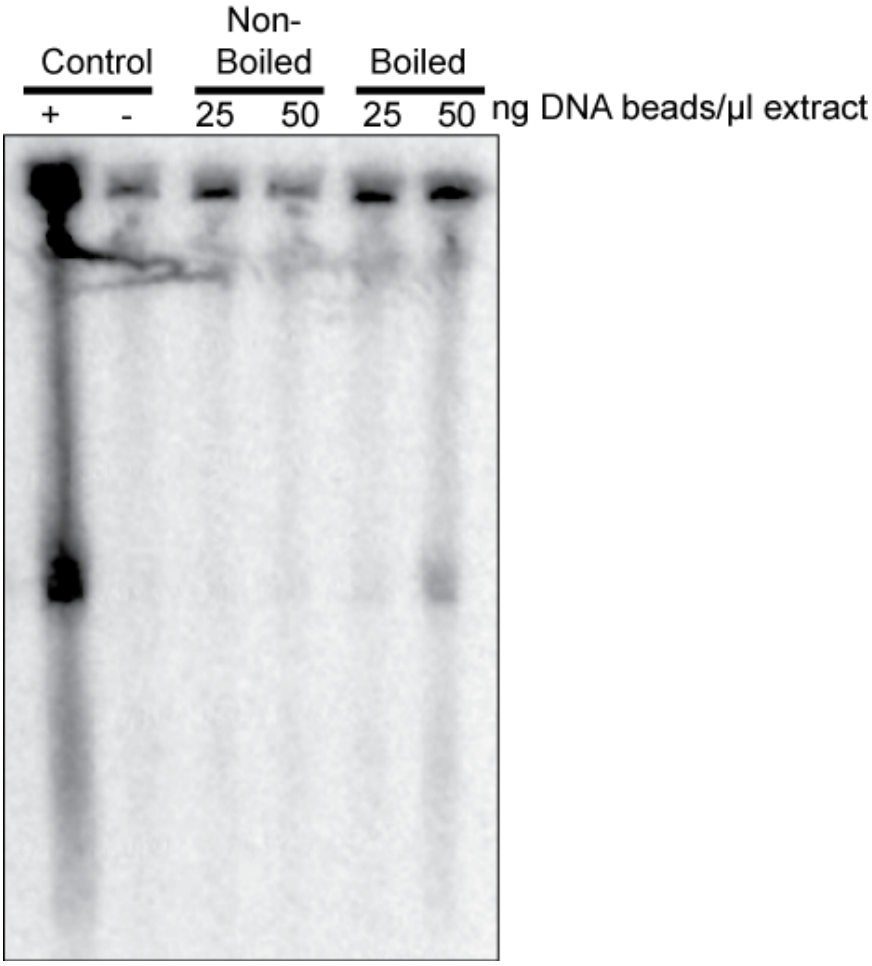

Fig. S4. Inhibitory activity can be removed from extract-treated DNA. DNA-beads were exposed to crude extract and then boiled or left on ice. DNA-beads that had been boiled for 10 minutes regained their ability to titrate out factor in a fresh extract indicating that boiling destroyed the inhibitory factor.

Fig. S5

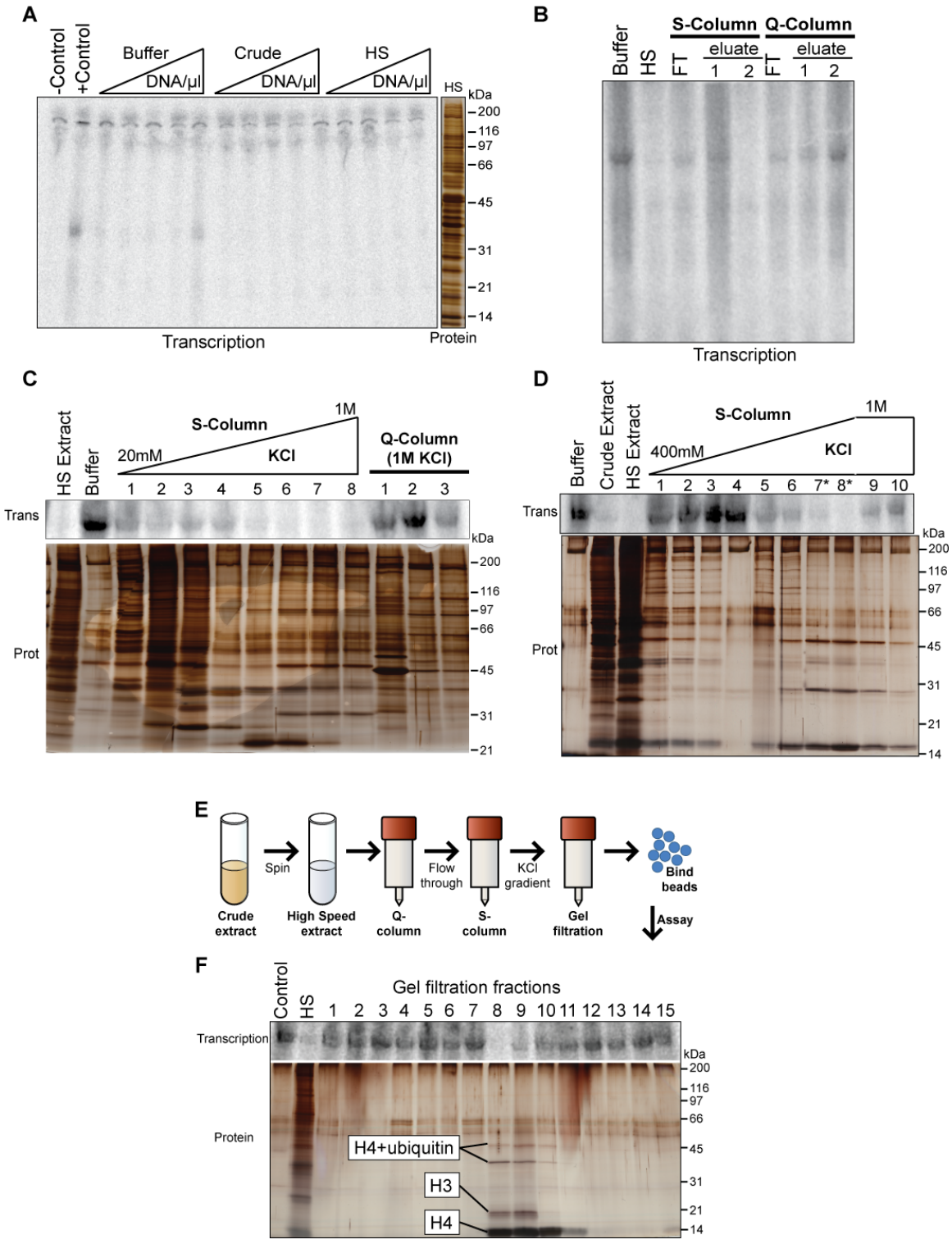
A
-Control
+Control
Buffer
DNA/µl
Crude
DNA/µl
HS
DNA/µl
HS
kDa
200
116
97
66
45
31
21
14
Transcription
Protein
B
Buffer
HS
S-Column
FT
eluate
1
2
Q-Column
FT
eluate
1
2
Transcription
C
HS Extract
Buffer
20mM
S-Column
KCl
1M
1 2 3 4 5 6 7 8
Q-Column
(1M KCl)
1 2 3
Trans
Prot
kDa
200
116
97
66
45
31
21
D
Buffer
Crude Extract
HS Extract
400mM
S-Column
KCl
1M
1 2 3 4 5 6 7* 8* 9 10
Trans
Prot
kDa
200
116
97
66
45
31
21
14
E
Crude extract
Spin
High Speed extract
Q-column
Flow through
S-column
KCl gradient
Gel filtration
Bind beads
Assay
F
Control
HS
Gel filtration fractions
1 2 3 4 5 6 7 8 9 10 11 12 13 14 15
Transcription
Protein
kDa
200
116
97
66
45
31
21
14
H4+ubiquitin
H3
H4

Fig. S5. Intermediate gels during biochemical purification. (*A*) Titration of DNA beads treated with buffer, crude extract, or high speed extract shows that both crude and high-speed extract are able to inhibit the ability of beads to induce transcription in a fresh extract. (*B*) Flow-through and elute of dilute high speed extract from Q- and S-columns bound in 20mM KCl and eluted with 1M KCl indicates that under these conditions the inhibitory factor binds the S-column but not the Q-column. (*C*) Flow through from Q-column in 20mM KCl directly bound by S-column. Fractions result from an 8-fraction linear gradient from 20mM to 1M KCl elution and the same Q-column eluted with 1M KCl. These results indicate that the inhibitory factor does not come off the S-column until high KCl concentrations and does not bind the Q-column. (*D*) Similar to (C), flow through from Q-column in 20mM KCl directly bound by S-column and was then washed with 400mM KCl. Fractions result from an 8-fraction linear gradient from 400mM to 1M KCl elution. The fractions marked with an asterisk were collected, pooled, concentrated, and run over a gel filtration column as in (F). (*E*) Schematic of the final resulting biochemical purification used to isolate the inhibitory factor. (*F*) The final output of the total purification protocol resulting from running fractions prepared as in (D) over a gel filtration column.

Fig. S6

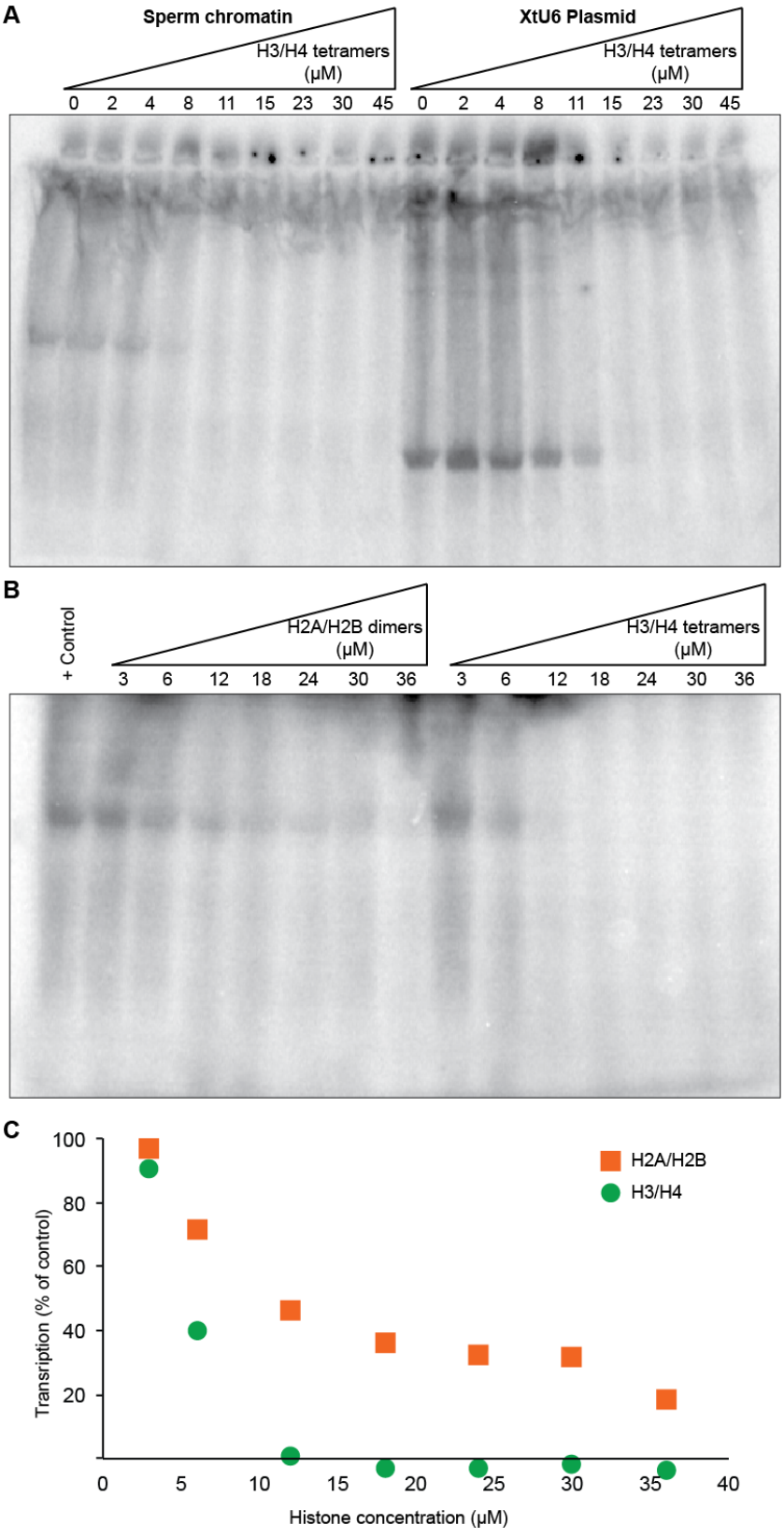
A
Sperm chromatin
H3/H4 tetramers (μM)
0 2 4 8 11 15 23 30 45
XtU6 Plasmid
H3/H4 tetramers (μM)
0 2 4 8 11 15 23 30 45
B
+ Control
H2A/H2B dimers (μM)
3 6 12 18 24 30 36
H3/H4 tetramers (μM)
3 6 12 18 24 30 36
C
Transcription (% of control)
100
80
60
40
20
0 5 10 15 20 25 30 35 40
Histone concentration (μM)
H2A/H2B
H3/H4

Fig. S6. H3/H4 inhibits transcription. (*A*) H3/H4 tetramers are able to inhibit transcription from *Xenopus* U6 plasmid DNA indicating that the observed effect is not specific to sperm DNA. (*B*) H2A/H2B dimers were also able to inhibit transcription, but not as efficiently as H3/H4 tetramers. (*C*) Quantification of the autoradiograph in (B). H3/H4 tetramers are approximately twice as efficient at inhibiting transcription as H2A/H2B dimers (as determined by how much is needed to reduce transcription from sperm chromatin by 50%). Even at the highest concentrations assayed, the inhibition from H2A/H2B is incomplete.

Fig. S7

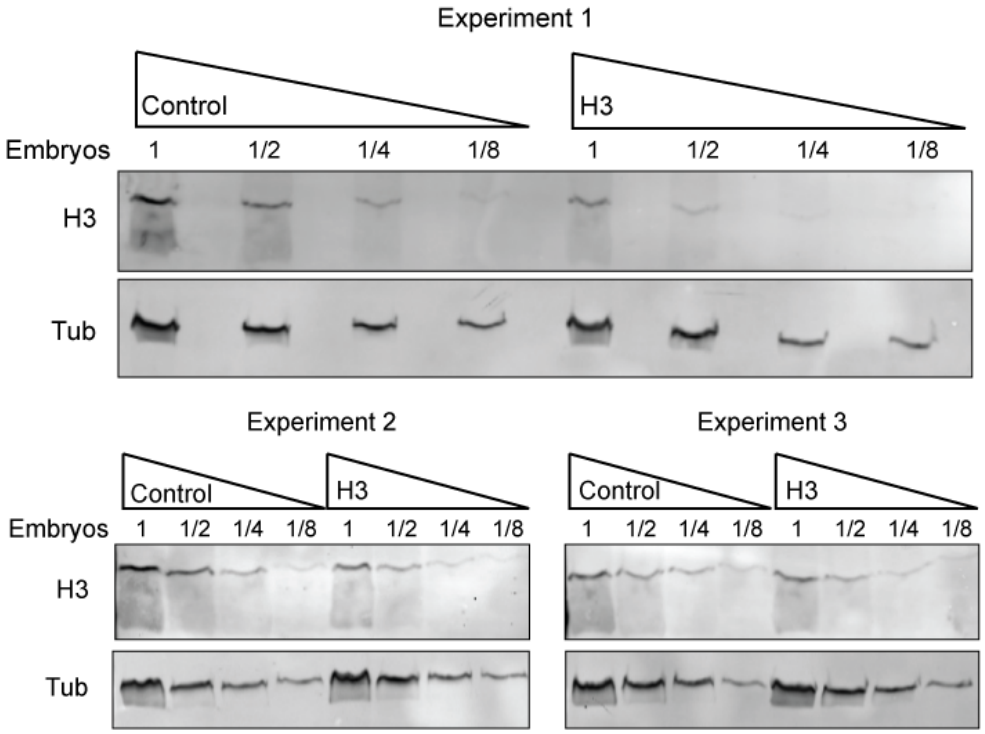

Fig. S7. H3 morpholinos reduce H3 concentrations at the MBT. Dilution series of control-morpholino-injected and H3 morphant embryos collected at 7.5 hours post-fertilization for the three clutch-matched experiments shown in Fig. S9. Embryos produced 56, 41, and 40% reduction in H3 (normalized to tubulin loading controls) in experiments 1, 2, and 3, respectively, as compared to control-injected embryos.

Fig. S8

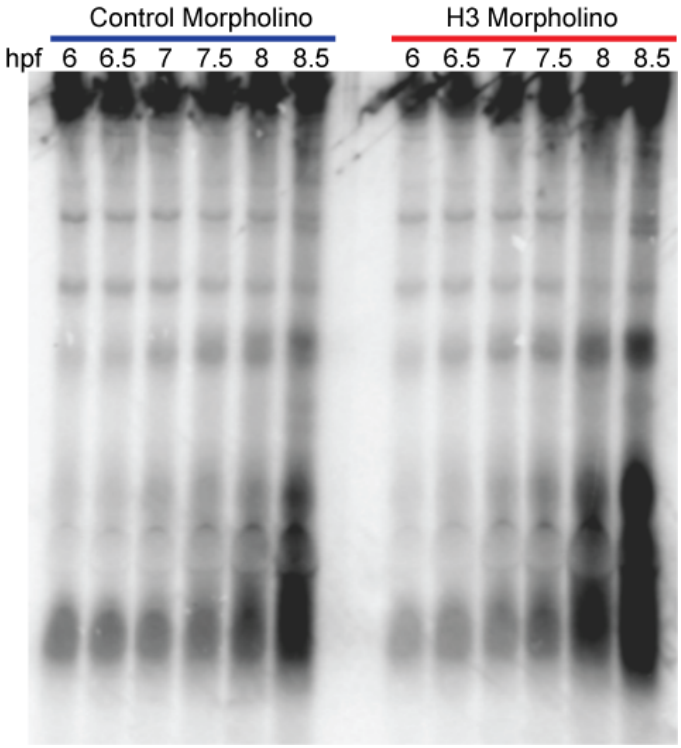

Fig. S8. H3 morphant embryos display increased transcriptional activation prior to the MBT compared to controls. Representative gel of total cumulative zygotic transcription in control morpholino compared to H3 morpholino embryos, assayed every 30 minutes starting at 6 hr post-fertilization. The MBT as defined by cell cycle lengthening occurs at 7.5-8 hours post-fertilization. Note that some zygotic transcription occurs prior to 6 hr post-fertilization in both control and experimental embryos.

Fig. S9

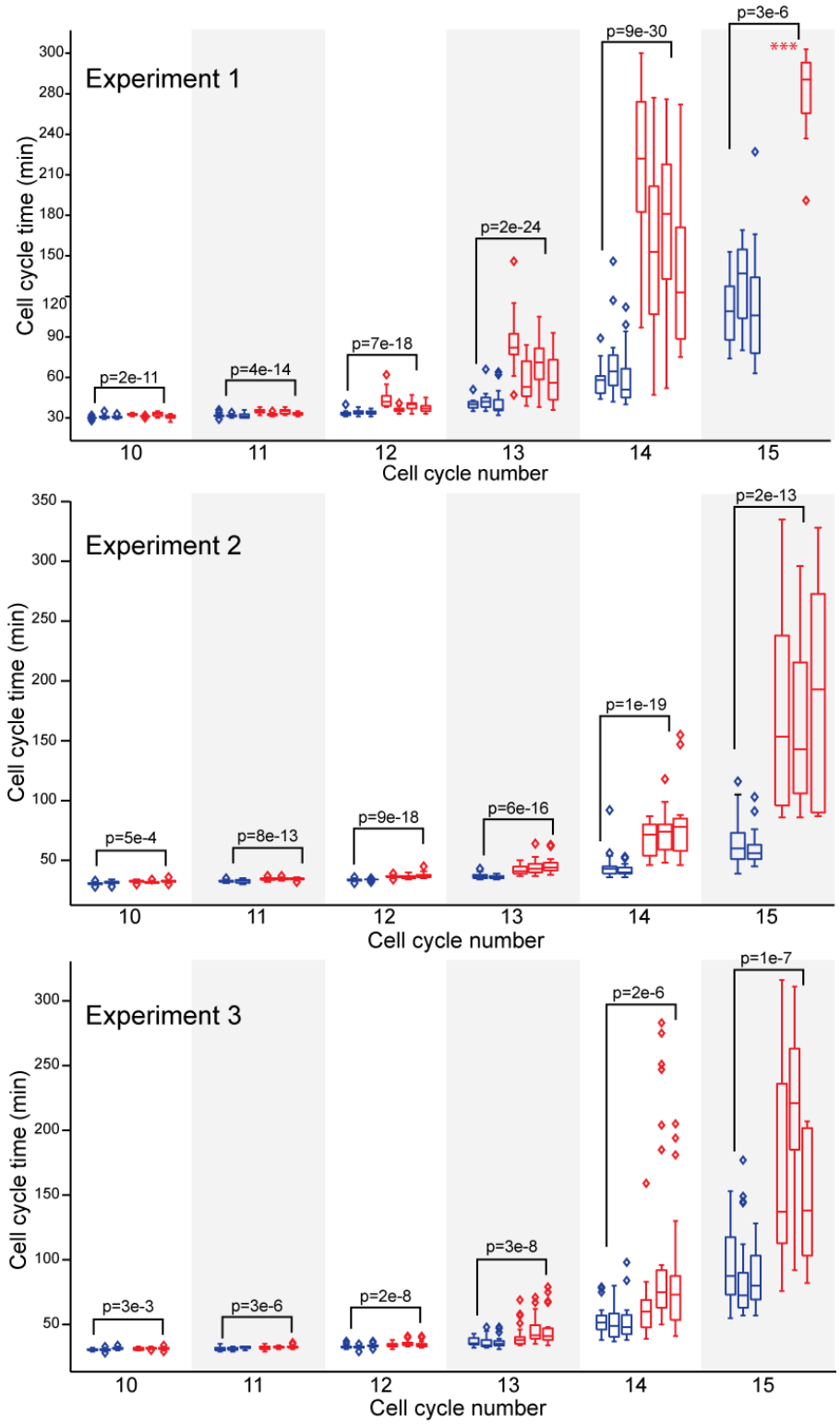
Experiment 1
Cell cycle time (min)
Cell cycle number
p=2e-11
p=4e-14
p=7e-18
p=2e-24
p=9e-30
p=3e-6
***
Experiment 2
p=5e-4
p=8e-13
p=9e-18
p=6e-16
p=1e-19
p=2e-13
Experiment 3
p=3e-3
p=3e-6
p=2e-8
p=3e-8
p=2e-6
p=1e-7

Fig. S9: H3 morphant embryos advance cell cycle lengthening in multiple independent experiments. Three independent clutches with 2-3 control embryos and 3-4 H3 morphant embryos. A minimum of 15 cells was manually counted from each embryo from movies with a frame rate of 1 frame per minute. All single cells counted descended from different lineages from the 9^{th} cell cycle onwards. All experiments show early cell cycle lengthening in the morphant embryos as compared to controls from the same clutch. Experiment 1 is also displayed in Fig. 6E.

Fig. S10

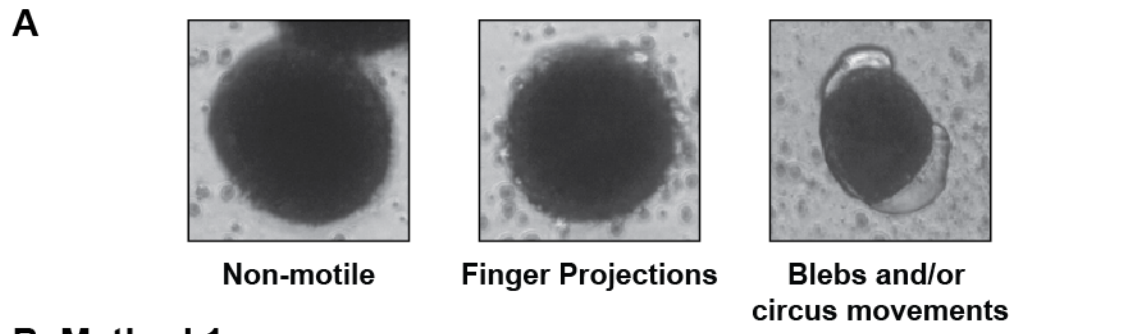
A
Non-motile
Finger Projections
Blebs and/or
circus movements
B Method 1
100
80
60
40
20
0
% of cells
6:00
6:45
7:00
7:15
7:30
7:45
8:00
8:30
9:00
Time post fertilization
Blebs/Circus
Finger projections
Control
H3 Morpholino
C Method 2
100
80
60
40
20
0
% of cells
6:00
6:30
7:00
7:30
8:00
8:30
9:00
Time post fertilization
Blebe/Circus
Finger projections
Control
H3 Morpholino

Fig. S10. Onset of cell motility is not advanced in H3 morphants. (*A*) Representative images of dissociated cells originating from control embryos categorized as non-motile, finger projection, or blebs and/or circus movements. See Supporting Movie 2 and 3 for dissociated cells from control and H3 morphant embryos respectively exhibiting these behaviors. (*B*) Percent motile cells from control and H3 morphant embryos dissociated at the 16-32 cell stage. Dissociated cells continued to divide and were assayed for motility using time lapse microscopy at indicated time points. Using this method, only 10-30% of dissociated embryos survive until the desired stage, consistent with (2). We therefore employed an alternate dissociation procedure in panel (*C*), where dissociation was performed just prior to imaging. See methods for a complete description. Both methods show that H3 morphant and control embryos have a similar percentage of motile cells at all time points between. 450 > N > 20 cells for each time point. Error bars denote SEM.

Fig. S11

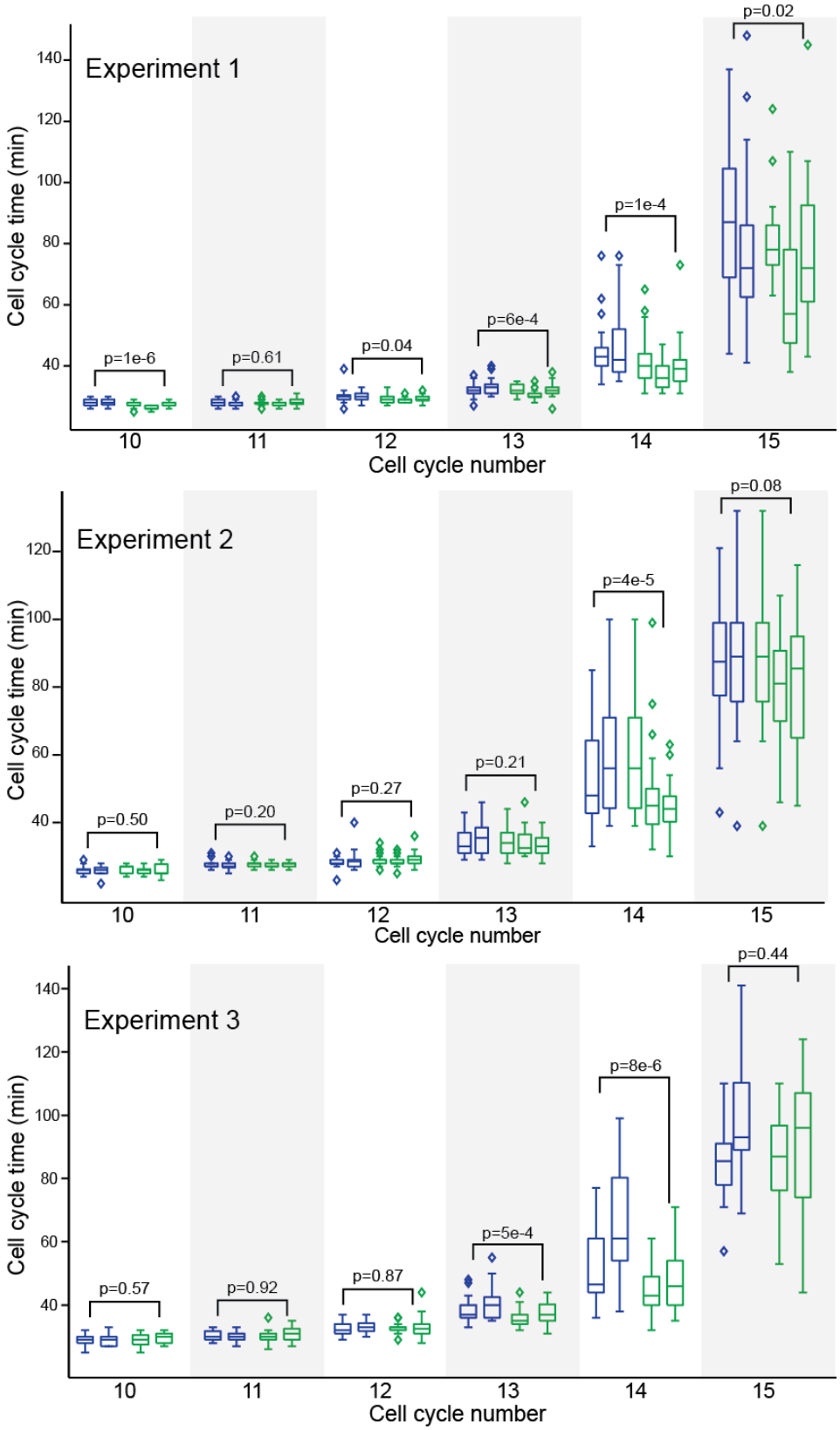
Experiment 1
Cell cycle time (min)
Cell cycle number
p=1e-6
p=0.61
p=0.04
p=6e-4
p=1e-4
p=0.02
Experiment 2
p=0.50
p=0.20
p=0.27
p=0.21
p=4e-5
p=0.08
Experiment 3
p=0.57
p=0.92
p=0.87
p=5e-4
p=8e-6
p=0.44

Fig. S11. H3H4 shortens the first post-MBT divisions in multiple independent experiments. Three independent clutches with two control embryos and 2-3 H3/H4 injected embryos. Cell cycle durations were measured as described in the methods. Experiments 1 and 2 were injected with 1.1ng/nl H3/H4 tetramers and experiment 3 was injected with 1.4ng/nl H3/H4 tetramers in 50% CSF-XB. Experiments 1 and resulted in a 24% and a 12% increase in H3 respectively as measures by Western blot 7.5 hr post-fertilization. Controls were injected with 50% CSF XB. Experiment 1 is also displayed in Fig. 7.

Supplemental Table: Mass spectrometry results

Band	Protein ID	Type	Number of hits
1	H4_XENLA	H4	14
1	H32_XENLA	H3	6
1	H2B11_XENLA	H2B	3
1	H33_XENLA	H3	3
1	H2AV_XENLA	H2A	2
1	A2BDA0_XENLA	H4	2
1	H2AZL_XENLA	H2A	1
1	H2A1_XENLA	H2A	1
2	H32_XENLA	H3	16
2	H4_XENLA	H4	12
2	H2B11_XENLA	H2B	7
2	CENPA_XENLA	H3	5
2	Q6PH89_XENLA	H2A	3
2	H33_XENLA	H3	3
2	UBIQP_XENLA	Ubiquitin	3
2	Q6DKE3_XENLA	H2A	2
2	H2A1_XENLA	H2A	2
2	A2BDA0_XENLA	H4	1
2	Q3KQC9_XENLA	Ribosomal	1
3	H4_XENLA	H4	11
3	1433T_XENLA	12-3-3 theta	4
3	Q7T0R9_XENLA	Ribonuclear	4

3	UBIQP_XENLA	Ubiquitin	**4**
3	H32_XENLA	**H3**	**3**
3	RAN_XENLA	Ran GTPase	**3**
3	RS8_XENLA	Ribosomal	**3**
3	H33_XENLA	**H3**	2
3	RL10A_XENLA	Ribosomal	2
3	A2BDA0_XENLA	**H4**	1
3	PSA7A_XENLA	Proteasome subunit	1
3	Q6AZR7_XENLA	Proteasome subunit	1
3	Q8AVT2_XENLA	Ribonuclear	1
4	H4_XENLA	**H4**	**10**
4	Q7T0R9_XENLA	Ribonuclear	**5**
4	H32_XENLA	**H3**	**3**
4	UBIQP_XENLA	Ubiquitin	**3**
4	EF1B_XENLA	Elongation fact (translation)	1
4	A2BDA0_XENLA	**H4**	1
4	Q68A88_XENLA	Proteasome subunit	1

Supplemental table: Total results from mass spectrometry of bands shown in. 3B, including the number of unique reads identified for each protein.

Movie Captions:

Supplemental Movie 1: Representative embryos from the same clutch; injected with control morpholino (top left) and H3 morpholino (bottom right). Embryos divide synchronously until near the MBT when the H3 morphant embryo begins to slow prematurely. The cumulative effect of the longer cell cycles is that the H3 morphant embryo ends the movie with larger cells than the control embryo.

Supplemental Movie 2: Representative movie of dissociated control morpholino injected blastomeres 9 hours post fertilization. Note that at this time the majority of cells display blebs and/or circus movements.

Supplemental Movie 3: Representative movie of H3 morpholino injected blastomeres 9 hours post fertilization. Note that, much like control morpholinio embryos shown in supplemental movie 2, the majority of cells also display blebs and/or circus movements.